

GEOELECTRIC RESISTIVITY SOUNDING FOR GROUNDWATER EVALUATION: TWO FIELD EXAMPLES.

Yehia E. Abdelhady, Essam A. Morsy and Sherif M. Hanafy

Geophysics Dept., Faculty of Science, Cairo University

استخدام طريقة السبر الكهربائي لتقييم الخزانات الجوفية: مثالان تطبيقيان

الخلاصة: تم تطبيق طريقة السبر الكهربائي الرأسي في منطقتين مختلفتين بمصر بهدف تقييم خزان المياه الجوفي بكل منطقة، وتم ربط نوعية المياه ودرجة ملوحتها بقيم المقاومة النوعية لها حيث أن القيم المرتفعة للمقاومة النوعية تدل على انخفاض الملوحة للمياه الجوفية. في المثال الحقل الأول (بمدينة قنا الجديدة) تم قياس ١٠ جسات للسبر الكهربائي الرأسي باستخدام نظام شلمبرجير. ووجد ان الطبقات التحتسطحية تتكون من (١) طبقة سطحية من رسوبيات الوديان، (٢) طبقة متداخلة من الحصى والرمل، (٣) طبقة من الحجر الرملي الجاف، (٤) طبقة من الحجر الرملي المشبع بالمياه، (٥) طبقة غير منفذة من الحجر الرملي الطيني. وتمثل الطبقة الرابعة الخزان الجوفي بسلك يتراوح بين ٤٨-٦٢ متراً وعمق يتراوح بين ٢٨-٣٩ متراً شمال الموقع و عمق يتراوح بين ٥-٣٢ متراً جنوب الموقع. وتم تبرير غياب الطبقة الحاملة للمياه بشمال شرق الموقع نتيجة وجود صدع يمنع وصول المياه. ووجد أن المقاومة النوعية للطبقة الحاملة للمياه تتخفف باتجاه الجنوب مما يدل على ارتفاع ملوحة المياه، وذلك نتيجة البعد عن نهر النيل الذي يمثل المصدر الرئيسي للخزان الجوفي. وبالنسبة للمثال الحقل الثاني (منطقة الخطاطبة) تم قياس ٦ جسات كهربية، وتفسير وتحليل القراءات الحقلية وجد ان الطبقات التحتسطحية تتكون من (١) طبقة رمال جافة، (٢) طبقة رمل وحصى، (٣) طبقة رمل مضغوط، (٤) طبقة رمال مشبعة (٥) طبقة رمال مشبعة بمقاومة نوعية أقل من الطبقة الرابعة نتيجة زيادة الملوحة للمياه الجوفية بهذه الطبقة. وأن سمك الطبقة الحاملة للمياه (الطبقة الرابعة) يتراوح بين ٨-٦٩ متراً ويعمق متوسط يصل الي ٦٨ متراً من سطح الأرض.

ABSTRACT: Geoelectric resistivity technique is applied in two different areas in Egypt to detect and evaluate the quality of subsurface groundwater aquifers. As it is well known the higher the resistivity values the lower the salinity and the better the water quality for agricultural purposes. In the first field example (New Qena city) 10 VES stations are conducted using Schlumberger array. The subsurface column consists of 5 resistivity layers. The first layer is a surface layer composed of very dry wadi deposits, followed by an intercalation layer of gravel and coarse sand, then a dry gravely sandstone, and a saturated sandstone layer, then an impermeable clayey sandstone. The aquifer is represented by the fourth layer with a thickness ranging between 48–62m at depth of 28–39m at the northern part and 5–32m at the southern part of the area. The absence of the aquifer at the northeastern part is attributed to faulting. The aquifer resistivity decreases towards the southern part of the area due to the increasing saline content and increasing distance from the river Nile (main recharging source). In the second field example (El-Khatatba area) a total of 6 Schlumberger VES stations are conducted in the area. The interpretation of the conducted data yields 5 subsurface layers, a thin surface dry loose sands, a coarse sand-gravel layer, a compacted sand layer, a saturated sandstone layer (represents the aquifer), and a saturated sandstone layer with lower resistivity values due to higher saline content. The thickness of the aquifer is 8–69m, while its average depth is 68m.

INTRODUCTION:

The major problem facing the construction of new communities or development of arid or semiarid areas is the source of water. Groundwater is considered as one of the main sources of water, particularly in the desert areas. The present study is an attempt to use the earth resistivity method in investigation of groundwater in two desert areas; New Qena city and El-Khatatba area.

Electrical sounding surveys are usually designed to measure the electrical resistivity of subsurface materials and to discriminate between anomalies which are indicative of subsurface electrical resistivity contents associated with lithologic and/or hydrologic characteristics (Denahan and Smith, 1984; Senosy, 1997) by making measurements at the earth surface. Its inherent capability is to detect changes in electrical conductivity of subsurface layers that reflect the fluid content of such layers (Jakosky, 1950; Weaver, 1929). Therefore it is an important tool for groundwater

exploration. Schlumberger field array is usually used because it has proven effective for groundwater exploration (Edwards, 1977; Zohdy et al., 1984).

In the two field examples 16 VES stations (10 in the first one and 6 in the second) are conducted using the Syscal R2 system. The Schlumberger configuration is used in all conducted VES stations. The main target of this study is to qualify the subsurface water aquifer for agricultural purposes. Thus the depth, thickness, and quality of the subsurface groundwater aquifer as well as the P factor are found in both areas. The P (Equ. 1) factor represents the aquifer resistivity – thickness product, where the bigger the P factor the better the groundwater quality (Zohdy, 1977).

$$P = hp \quad (1)$$

where; h is the thickness in meters and ρ is the true resistivity in Ω m.

NEW QENA CITY AREA

The first field example is carried out in New Qena city, Upper Egypt, between latitudes $26^{\circ} 11 - 26^{\circ} 16$ N and longitudes $32^{\circ} 43 - 32^{\circ} 46$ E (Fig. 1). The maximum AB/2 of the conducted 10 VES stations is 450 m. The field data is interpreted through three steps; (a) smoothing of the field data curve during data acquisition where sharp peaks are neglected. Such peaks are difficult to interpret and cause ambiguity in the interpretation results, (b) preparing an initial model depending on the geological background as well as previously drilled wells, and (c) introducing the initial models into the Van Der Velpen (1988) software. More than one iteration were used to reach the best fit between the smoothed field curve and the calculated one. The RMS error of the resulted models ranges between 1.5-5.9%. Figure (2) is an example (VES # 2) of the conducted data after final interpretation processes.

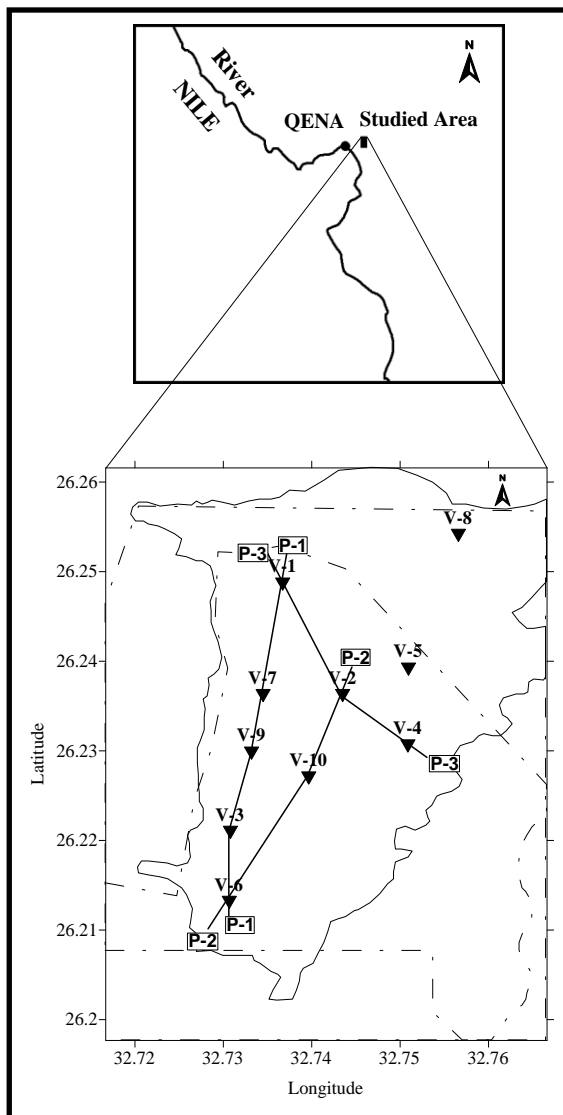


Figure 1: A location map showing the area of study (first field example), the locations of the conducted VES stations, and the location of the geoelectric cross-sections.

Field Data Interpretation

The field data acquisition was carried out during the summer season where the temperature is over 47°C during day time, which causes an increase of the earth's surface resistance to values over 900 k.ohm. This problem is overcome by using long electrodes buried in small holes, which are filled with highly saline solutions. The interpreted VES stations are used to produce three geoelectric cross sections (Fig. 3). A total of 5 subsurface layers are recognized in the geoelectric cross sections (naming them is controlled by a drilled borehole (Fig.1)) as follows:-

1. A surface layer composed of very dry wadi deposits (sand or gravelly sand). It has a resistivity > 10000 ohmm and a thickness ranging between 0.3–1.9m.
2. Intercalation layer of gravel and coarse sand with resistivity ranging between 372–780 ohmm and thickness ranging between 7.2–8.9m.
3. A dry gravelly sandstone of resistivity 1300–3200 ohm m and thickness 5–36.5m.
4. A saturated sandstone layer, which forms the main subsurface aquifer. In the northern part (VES stations # 1, 2, and 7) the true resistivity ranges between 107–180 ohmm, with a thickness ranging between 48-62m and a depth to its top between 28–39m. In the southern part (VES stations 3, 4, 6, 9, and 10) the true resistivity ranges between 23–46 ohmm with a thickness of about 48 m and a depth of 5–32m. The aquifer is not represented in VES stations 5 and 8.
5. An impermeable clayey sandstone with resistivity > 1000 ohmm.

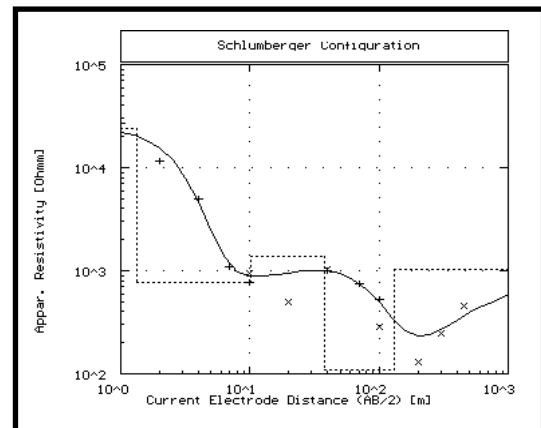


Figure 2: An example of the acquired field data (VES # 2).

Figures 4a, b, c, and d show the contour maps of the depth, thickness, true resistivity, and P factor of the subsurface aquifer. The depth to the aquifer increases towards the southwestern part of the study area, starting with 5m and increasing to about 60m (Fig. 4a). The thickness of the aquifer increases towards the western side of the area and reaches 64.5m at VES station 9 (Fig. 4b). The true resistivity decreases towards the south and

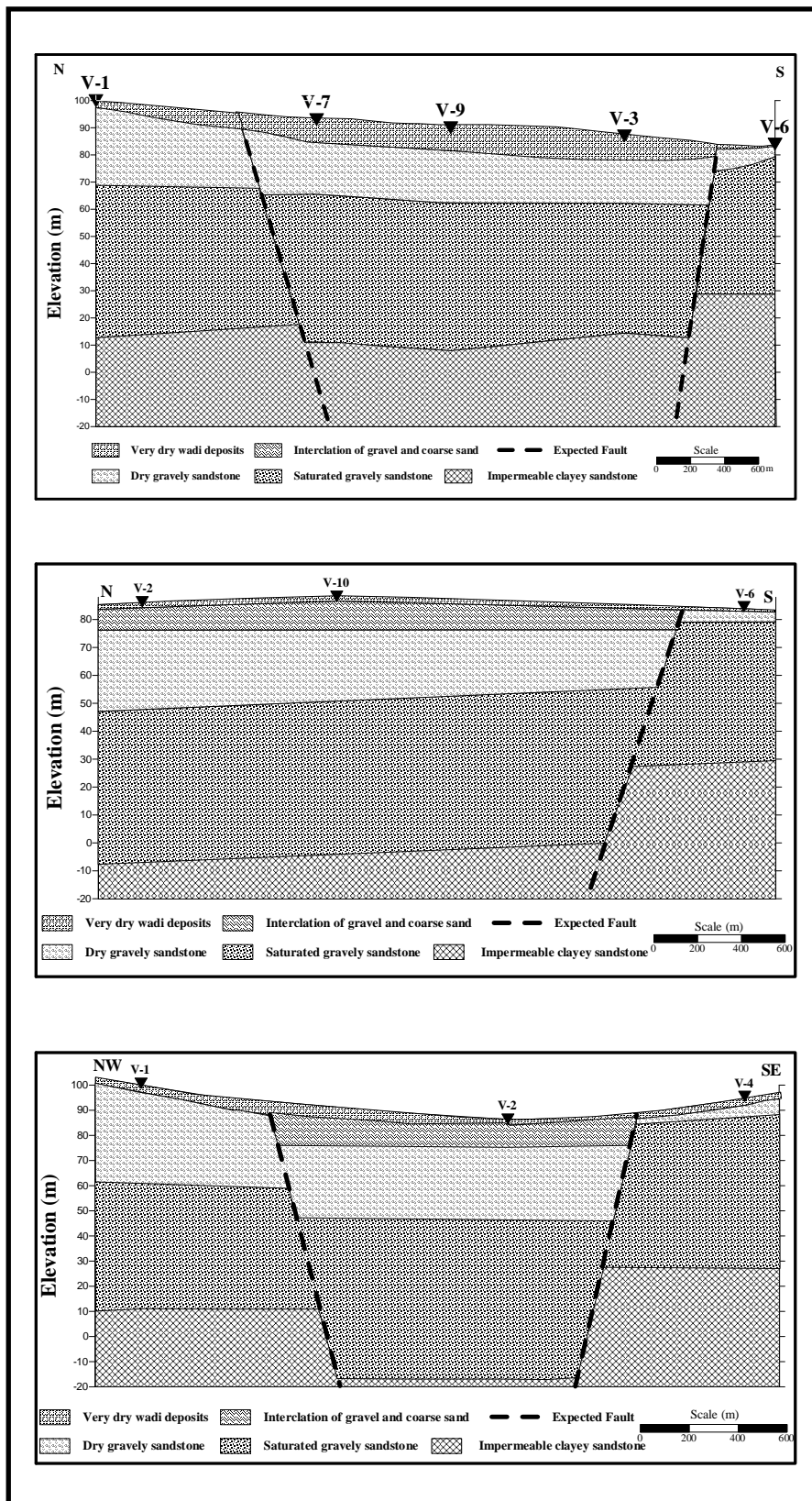


Figure 3. The geoelectric cross-sections P1, P2, and P3 of the first field example (New Qena city).

the southeastern parts of the study area, where the maximum resistivity value is 178.9 ohmm at VES station 1, and the minimum is 23.9 ohmm at VES station 6 (Fig. 4c). The P factor increases towards the northwestern corner of the study area, where it reaches 8500 ohm.m² (Fig. 4d), representing the best location for producing groundwater.

The absence of the aquifer in the northeastern part of the study area (VES stations 5 & 8) structural regime

in the form of faulting that affects the saturated area and prevents groundwater from moving towards the northeast by bringing the impermeable clayey sandstone layer to a very shallow depth. The shallowness of the groundwater aquifer at the southern part (VES stations 4 and 6) can be interpreted as being due to another main fault, which passing between VES stations 3 and 6, 6 and 10, and 2 and 4. This fault is running in the SW – NE direction.

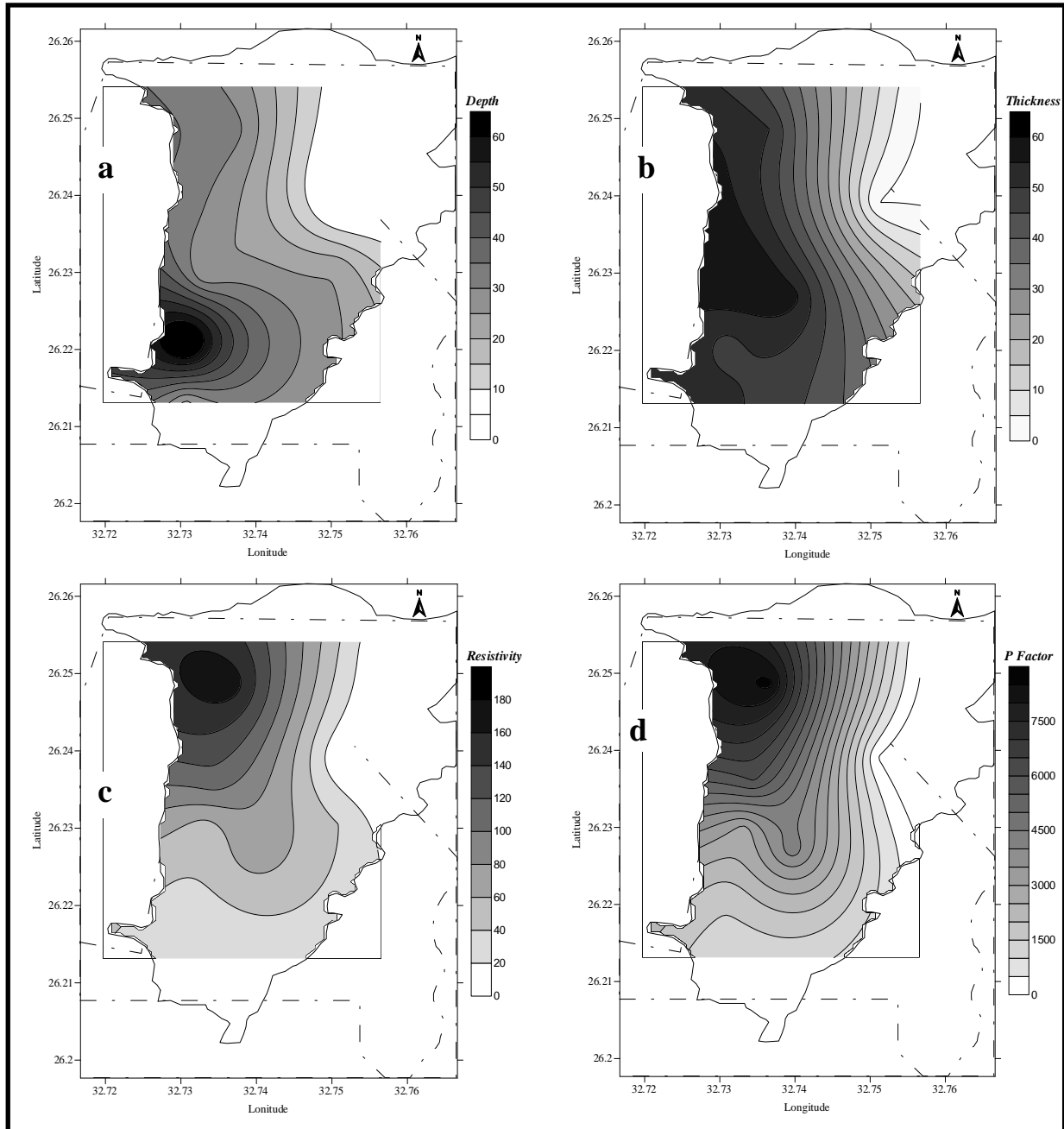


Figure 4: Four countour maps showing (a). the depth, (b). the thickness, (c). the resistivity, and (d). the P factor of the subsurface water aquifer.

EL-KHATATBA AREA

The second field example is carried out in El-Khatatba area, to the north of the Western Desert, Egypt, at latitude 30° 00 N and longitude 30° 20 E. The maximum AB/2 of the acquired 6 VES's is 600m except VES station 2 where maximum AB/2 is 200m because of bad field conditions (Fig. 5).

Field Data Interpretation

The 6 VES curves (Fig. 5) are interpreted following the same three steps used in New Qena city. An example of the acquired data and its interpretation is shown in Figure (6). The resulting geoelectric models are used to produce 2 geoelectric cross sections (Fig. 7), which show the presence of 5 subsurface geoelectrical layers, namely:

1. A thin surface layer represented by loose sand with resistivity ranging between 12–40 ohmm and thickness between 1.2-2.7m.
2. A coarse sand-gravel layer with resistivity ranging between 24–160 ohmm and thickness between 8–20m.
3. A compacted sand layer with relatively high resistivity values ranging between 267-566 ohmm and thickness between 3-60m.
4. A saturated sandstone layer (the aquifer) with resistivity ranging between 32-190 ohmm and thickness between 8-69m. The depth to the top of the aquifer ranges between 54-71m from the ground surface.
5. A saturated sandstone layer with lower resistivity values due to higher saline content, where the resistivity ranges between 15-28 ohmm.

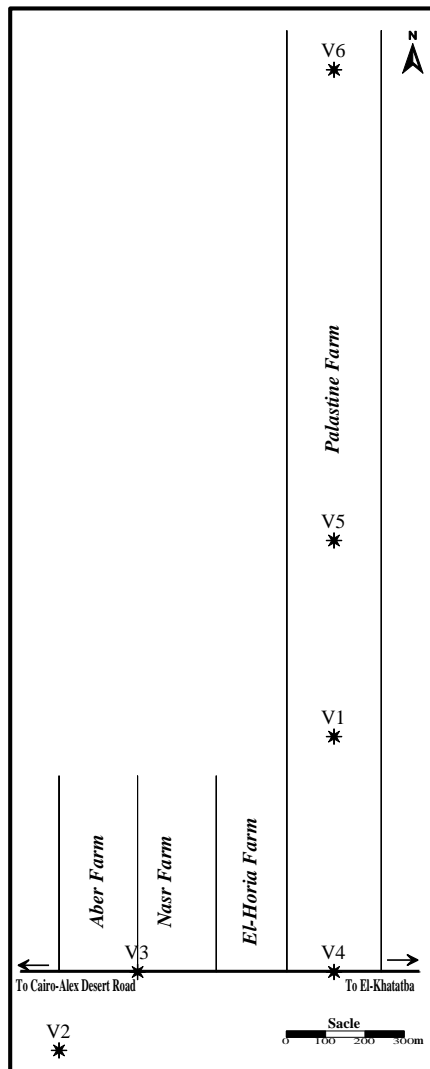


Figure 5: A location map shows the area of study (second field example) and the locations of the conducted VES stations.

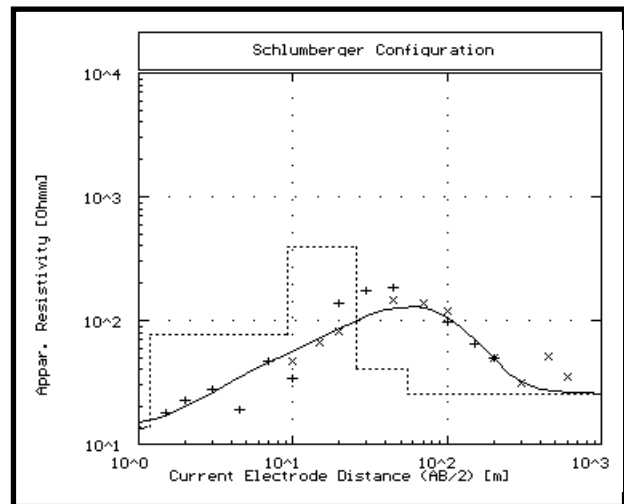


Figure 6: An example of the acquired field curve (VES # 2).

Figure (8) shows 4 contour maps representing the depth, thickness, resistivity and the P factor of the subsurface aquifer. The depth to the top of the aquifer increases from 20 to 68.2m towards the southwestern corner of the study area (Fig. 8a). The thickness of the subsurface aquifer increases towards the southwestern corner, reaching 68.7m (Fig. 8b). The high resistivity values are concentrated in the southern part of the site, and interpreted as indicative of more fresh water than the northern and western parts of the study area (Fig. 8c). The P factor reaches its maximum value 12000 ohm.m² at the southwestern corner of the study area. This is the best location for drilling a producing water well because of the high thickness and high resistivity values obtained (Fig. 8d).

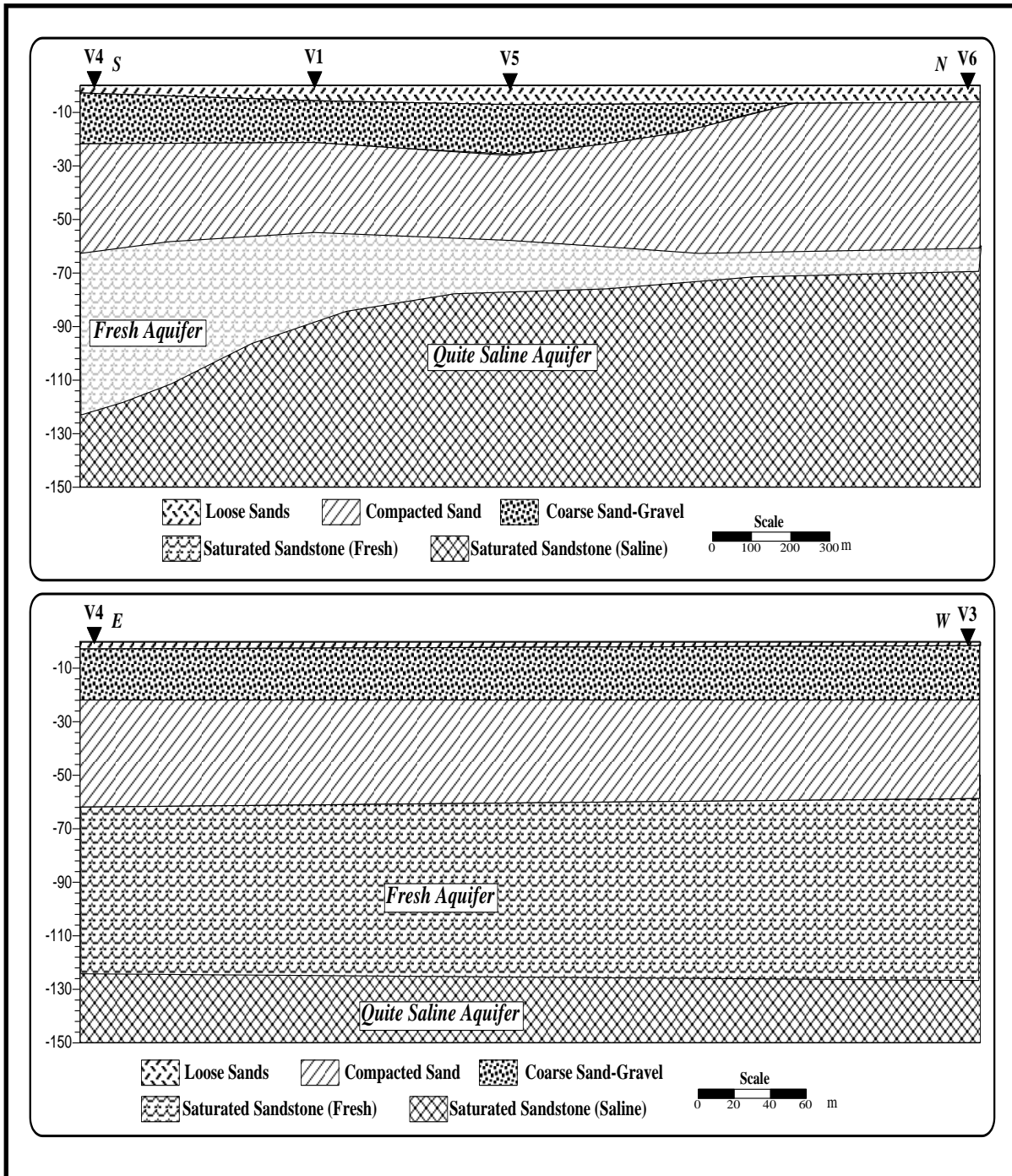


Figure 7. The geoelectric cross-sections P1 and P2 of the second field example (El-Khatatba).

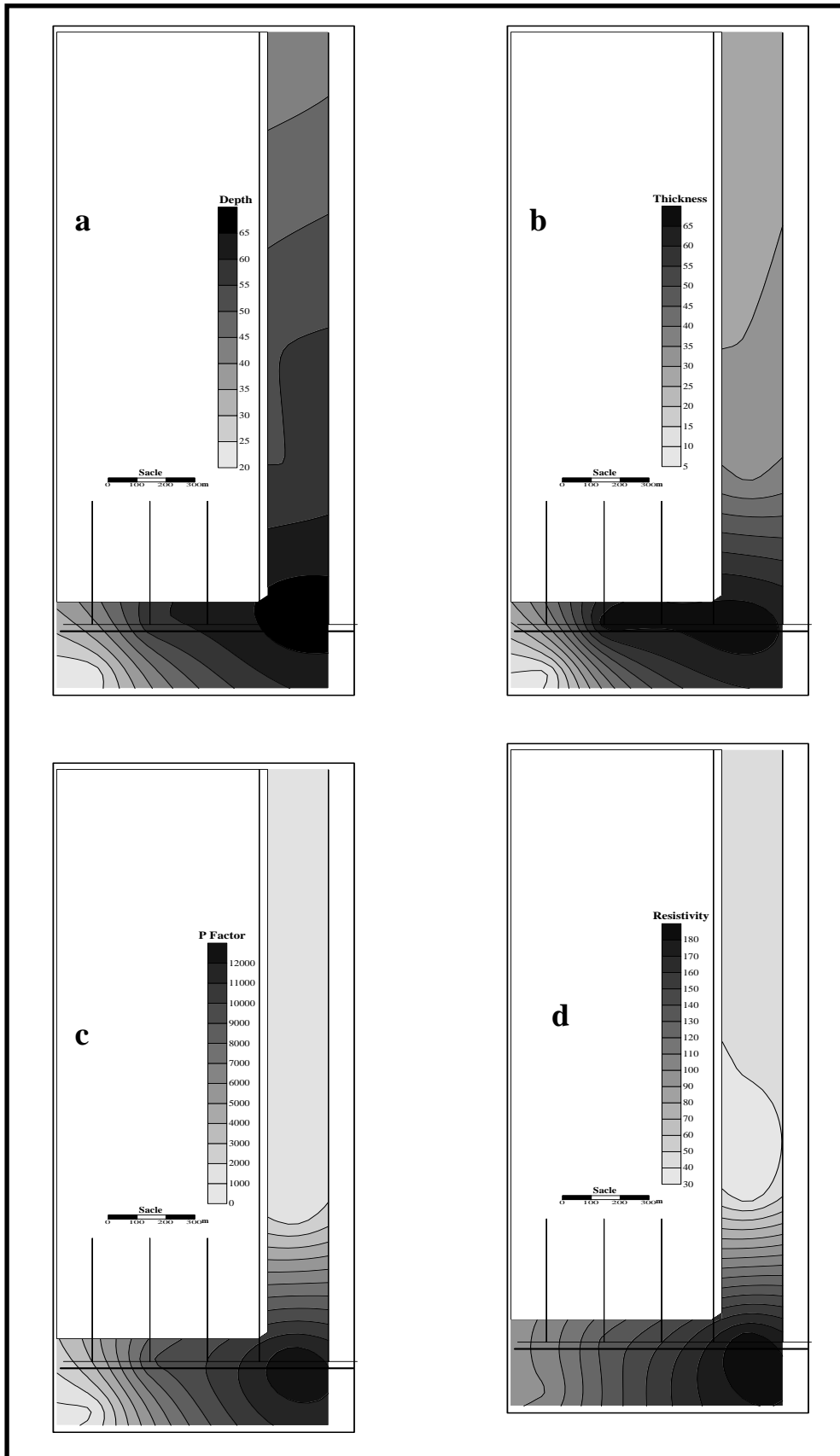


Figure 8: Four contour maps showing (a) the depth and (b) the thickness of the subsurface water aquifer (c) the resistivity and (d) the P factor of the subsurface water aquifer.

CONCLUSIONS

First field example

- a. The geoelectric subsurface consequence consists of 5 distinctive geoelectrical layers; a surface layer composed of very dry wadi deposits, an intercalation layer of gravel and coarse sand, a dry gravelly sandstone layer, a saturated sandstone layer, and an impermeable clayey sandstone.
- b. The aquifer is represented by the fourth geoelectrical layer. In the northern part its thickness ranges between 48–62m with resistivity ranging between 107-180 ohmm and depth to the top of 28–39m. At the southern part the aquifer thickness is about 48m, the depth to the aquifer's top is 5–32m, and the resistivity values between 23–46 ohmm.
- c. The aquifer is missing in the northeastern part of the study area, especially under VES locations 5 and 8. This is due to the presence of a major fault that bring the impermeable clayey sandstone layer to shallow depth and precludes the groundwater from moving in the northeastern direction.
- d. The aquifer is very shallow in the southeastern part of the study area (VES locations 4 and 6). This is due to another fault with its upthrown side towards southeastern part of the area.
- e. The best location for groundwater well is the northwestern part of the study area.

Second field example

- a. The subsurface geoelectrical sequence consists of 5 different layers, namely; a thin surface dry loose sands, a coarse sand-gravel layer, a compacted sand layer, a saturated sandstone layer, and a saturated sandstone layer.
- b. The fourth and fifth layers form together the aquifer. The salinity of the fifth layer is higher than that of the fourth layer (the resistivity of the fifth layer is lower than that of the fourth). The thickness of the fresher aquifer (fourth layer) is 8–69m, while its average depth is 68m.
- c. The best location for groundwater well is the southern part of the study area.

REFERENCES

- Denahan, B. J . and Smith, D. L., 1984**, Electrical resistivity investigation of potential cavities underlying a proposed ash disposal area: *Environ, Geol.*, 6, p. 45-49
- Edwards, L. S., 1977**, A modified pseudosection for resistivity and IP: *Geophysics*, Vol. 42, No. 5, P. 1020-1036.
- Jakosky, J.N., 1950**, *Exploration Geophysics*: Los Angeles, Trija, 1,195 p.
- Senosy, M. M., 1997**, Ground water possibilities using earth resistivity method in some desert areas of Assiut province, Egypt: *Bull. Fac. Sci., Assiut Uni.*, 26(2-F), P. 169-187.
- Weaver, W., 1929**, Certain application of the surface potential method: *A.I.M.E. Geophys. Prosp. Trans.*, V. 81, P. 68-86.
- Zohdy, A. A. R., Eaton, G. P., and Mabey, D. R., 1974**, Application of surface geophysics to ground-water investigations: *Tech. of Water Sources, Investigation of U.S. Geol. Surv.*, Book 2.
- Zohdy, A. A. R., Eaton, G. P. and Mabey, D. R., 1984**, Applications of surface geophysics to ground-water investigations: Department of Interior US Geological survey, US Government printing office, Washington, Third printing, 116 p.
- Velpen, V, 1988**, ITC M.Sc. research project.

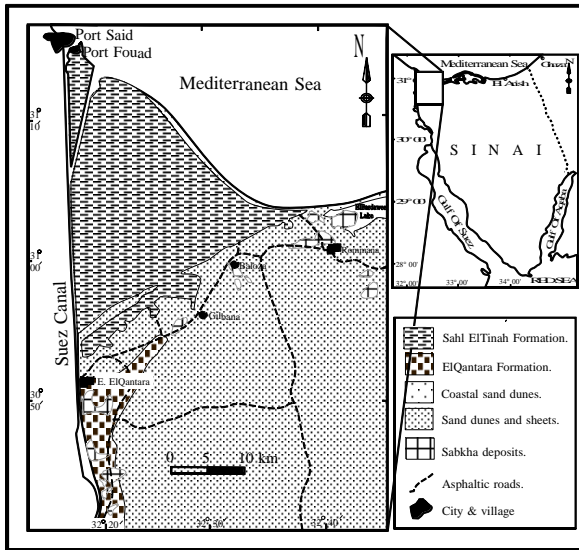


Figure 1. Geologic map of the study area (after ElHinnawi et al., 1994).

Data acquisition and processing

A reconnaissance field survey was planned to establish the location of the resistivity profiles taking into consideration the availability of boreholes in order to calibrate the resistivity data. The localities that are characterized by the presence of salt crust as well as surface water bodies were avoided.

In this respect, forty-nine Vertical Electrical Soundings (VES) were conducted in the study area using Schlumberger configuration. The main unit of TERRAMETER SAS 300C for measuring resistance and SAS 2000 as current penetration poster unit are used in the field survey. The VES stations are portrayed mainly along EW profiles, SW and SSE profiles (Fig. 2). The half distance between the potential electrodes ($MN/2$) was increased in steps, starting from 0.5 m to 20 m, in order to obtain a measurable potential difference. The current electrode half separation ($AB/2$) was usually increased in steps starting from 1 m to 500 m. It was not possible to intensify the VES stations in the area of study due to the rough nature of the area that is characterized by the presence of sand dunes and possible existence of dangerous mines that left behind the Egyptian-Israeli wars. Six VES stations were excluded because of their erratic behavior, which could refer to the high salinization in the locations.

Each VES was subjected to two different interpretation techniques; the first is the 1D-forward modelling, in which the iterative procedure of Zohdy (1989) was used (Fig. 3a). While the second is the 1D-inverse modelling (Fig. 3b), in which the weighted ridge regression scheme of Inman (1975), using the transformed thickness-resistivity model of Zohdy and Bisdorf (1979) as an initial model, was used. These models were performed in light of the lithologic and hydrogeological data of the boreholes and the results were presented in the form of cross-sections and maps.

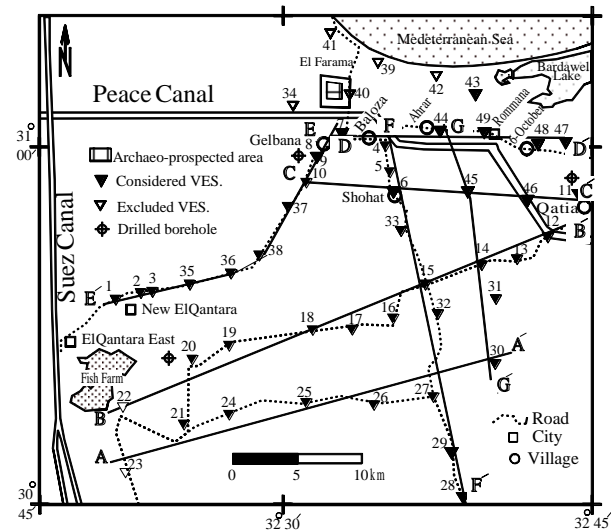


Figure 2. Location map of the VES station and the surveyed profiles in the study area

Calibration of VES Data

The geoelectric resistivity of sediments is one of the most variable physical properties, especially in a very complicated sedimentological environment that dominates such coastal areas (e.g. Ibrahim, 1998). Geoelectric resistivity depends mainly on the lithology, water content and salinity and there are no sharp guidelines to interpret the lithology and/or water content from the contrast in the resistivity layers. Therefore, the ambiguities in interpretation may occur and becomes very necessary to calibrate the observed VES data with the available borehole data. This enables assigning the geoelectric units to the corresponding lithologic units and consequently put a reliable control on the interpretation of the subsurface sequence in the study area. For this purpose, three vertical electric soundings have been carried out near to three drilled boreholes. These boreholes are Qatia, (quoted from Ewieda et al., 1992), Baloza (quoted from Stanley et al., 1996) and Qantara (drilled by the Suez Canal Authority). These boreholes were chosen (Fig. 2) to cover different sedimentological environments in the study area. The close correlation between the borehole data and the obtained resistivity models (Fig. 3) helped to assign resistivity ranges for the various lithologic units (Table 1) as a tool for subsurface geoelectric resistivity interpretation.

Rock unit	Resistivity range in
Fine sand saturated with brackish to saline water	50 to 155 ohm.m
Fine sand saturated with fresh water	155 to 385 ohm.m
Clay saturated with saline to brackish water	0.36 to 9.6 ohm.m
Silty to sandy clay saturated with saline to brackish water	10 to 50 ohm.m
Coarse sand gravels saturated with fresh water	≥ 500 ohm.m
Limestone conglomerate	≥ 700 ohm.m

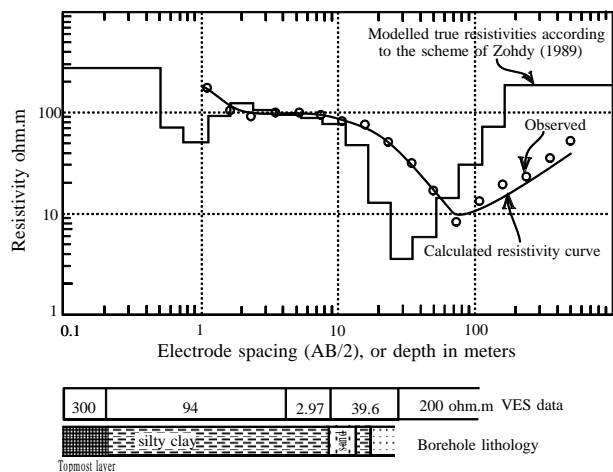


Figure 3. VES calibration with the lithology of the ElQantara bore hole in the area of study using A) forward modeling of Zohdy (1989) and B) inverse modeling of Inman (1985).

It is obvious that each lithologic unit is characterized by a wide range of resistivity which indicates that the lithology, salinity and water content play an essential role in relating the different resistivities to particular lithology.

RESULTS AND INTERPRETATION

In order to demonstrate the distribution of the litho-resistivity units, resistivities and thicknesses of each unit were used to construct detailed litho-resistivity cross-sections along the surveyed profiles. These cross sections show the broad distribution of geoelectric resistivities and their corresponding lithologic and hydrologic variations in the study area. Detailed interpretation of each cross section and the general correlation between resistivity layers, their thicknesses and depths along all sections, revealed that the subsurface geoelectric resistivity layers have a wide range of resistivities and can be classified into four main litho-resistivity units. It is found that all cross sections start with a thin topmost layer that attains variable resistivity with an average of 312 Ω.m and thickness ranging from 0.33 to 5.3 m with an average of 0.4 m. This resistivity zone is correspondent to the zone of aeration that is composed mainly of wet to dry, fine to coarse sand in the eastern and southern areas and becomes more silty and clayey in the northwestern parts. The wide range of resistivities that characterizes this topmost layer could be referred to the variations in the lithology and moisture content.

The second geoelectric resistivity unit is interpreted as a shallow sand aquifer that attains resistivity values decreasing generally northwards and varies from 72 to 385 Ω. m. The resistivity value of this aquifer is decreasing northwards giving an indication to an increase in the salinity of the groundwater. Its thickness generally decreases to the west and north and

increases southwards, ranging from about 4.5 to 33m. The critical correlation between the different litho-resistivity cross sections indicates that this shallow aquifer is present in the form of continuous layer in the south (Figs. 4), disconnected in the north (Fig. 5). In some areas this sand unit is intercalated with clayey lenses (Fig. 6) and absent in other localities (Fig. 7). Ewieda et al. (1992) mentioned that the direction of water flow in this aquifer is mainly towards the northwest direction and the fresh water was found as a thin layer floating over the saline water due to the direct rainfall during rainy seasons. In order to show the a real distribution of the shallow aquifer, the resulting thickness of this aquifer was used to construct the isopach map (Fig. 8) which indicates that the thickness of this aquifer ranges from 1.4 m in the northwest to reach about 60m in the extreme southeast showing a good agreement with the results of Ewieda et al. (1992).

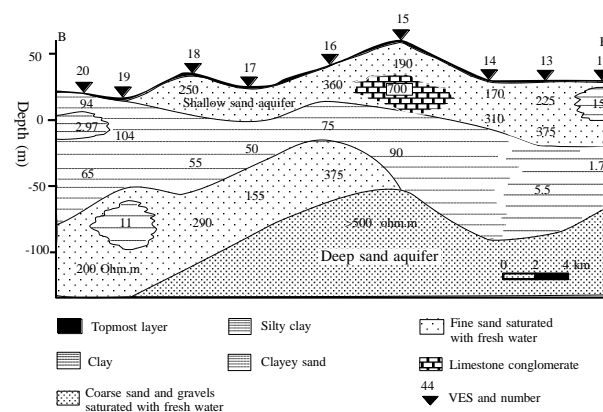


Figure 4. The shallow sand aquifer as a continuous layer.

The lowermost geoelectric resistivity unit that dominates the study area is characterized by its relatively high resistivity (exceeds 500 ohm.m) and depth ranging from 11.6 to 165m with an average 91m (Fig. 6). This high resistive layer is interpreted as a coarse sand and gravels layer saturated with fresh water that represents the Pleistocene deep sand aquifer in the study area. The fresh water of this Pleistocene aquifer is expected to be originating from the Pliocene aquifer that is connected with the Pleistocene shallow aquifer through fractures that characterize this area (Neev, 1977 and ElSayed et al. 2001). Based on the interpreted geoelectric cross sections, the depth from the ground surface to the top surface of this deep aquifer was calculated and used to construct the depth contour map of the deep sand aquifer (Fig. 9). This map shows that the depth to the surface of this aquifer ranges from 11.6 m at VES 38 to about 165m at VES 2 across profile E-É with an average depth of about 91m. Recently, REGWA drilled a well in the eastern part of the study area and the fresh water was encountered at 80m depth, which confirm the present results.

A thick clayey unit, ranging from clay to silty and sandy clay, separates the shallow and deep sand aquifers. This unit is characterized by a wide range of resistivities that vary from 0.38 to 50 ohm.m, reflecting the lateral inhomogeneity in its electrical properties that could be correlated to lithologic and hydrochemical variations. Towards the western part of the area, the resistivity of this unit decreases to less than 10 Ω. m (Fig. 5 and 7) that is interpreted as clay facies saturated with saline water. The great thickness of this clayey sediment to the west (Fig. 5) that reaches its maximum values of 180m, could be correlated with the flood plain sediments of the Nile Pelusium branch, which was extending in the NE direction to reach the sea at the present location of ElFarama area. In some parts of the study area, this clayey layer extends under a thin sandy cover and as tongues inside the sand at Baloza-Ahrar area and New Qantara-East. This phenomenon could be explained as the clay sediments were deposited in low topographic areas between high sand areas until the leveling of the surface is reached. Afterwards, the flooding clayey sediments continued to be deposited until the Pelusium branch, which carried these alluvial sediments to the area, is defunct. After the burial of the Nile branch, the area became a hosting area for sand that carried out by wind to cover these alluvial deposits.

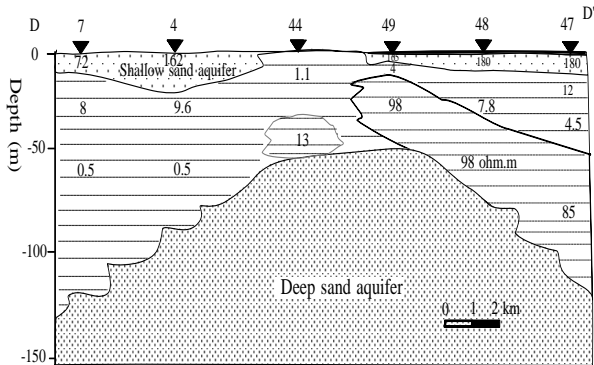


Figure 5. The shallow sand aquifer as disconnected layers in the northern areas and increasing the thickness of the clayey unit to reach its maximum value to the west.

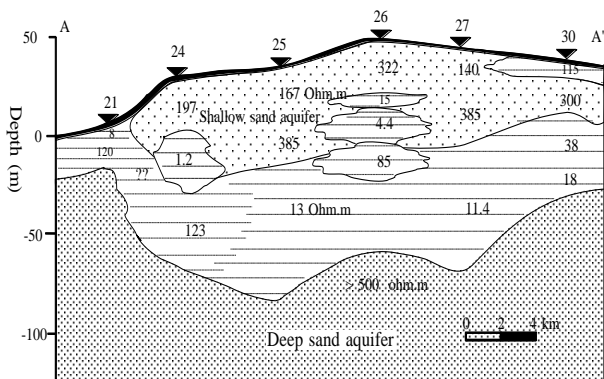


Figure 6. Shallow sand aquifer intercalated with clayey lenses.

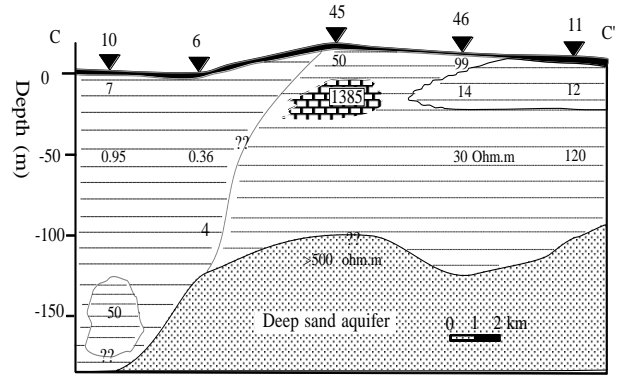


Figure 7. The absence of the shallow sand aquifer and a great thickness of clayey sediments, reaching its maximum value to the west.

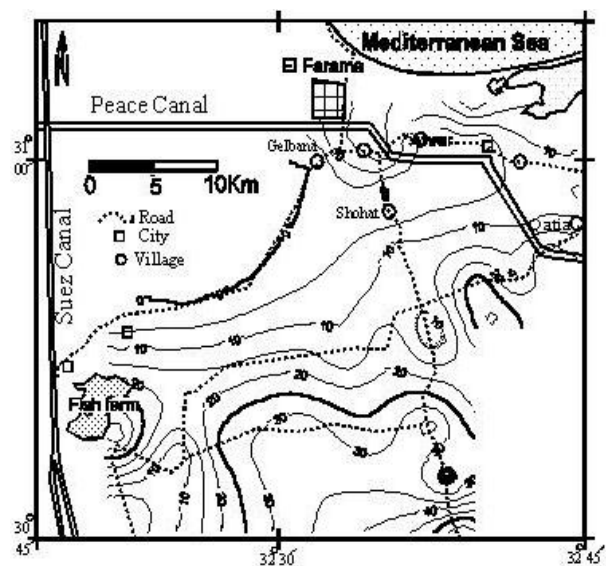


Figure 8. Isopach contour map of the shallow sand aquifer in the study area.

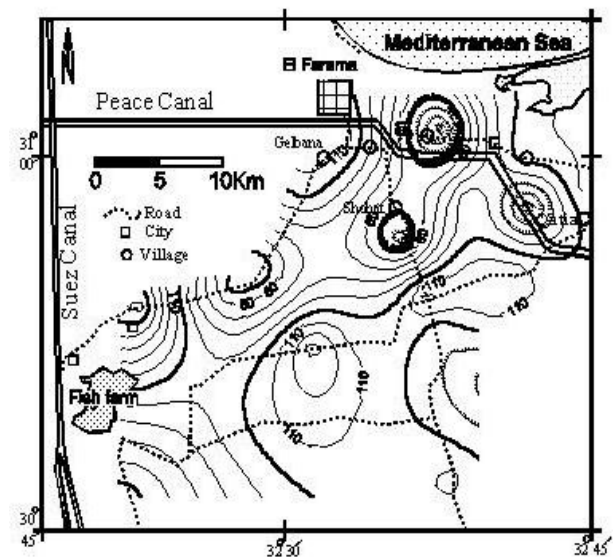


Figure 9. Contour map of the depth to the surface of the deep sand aquifer in the area of study.

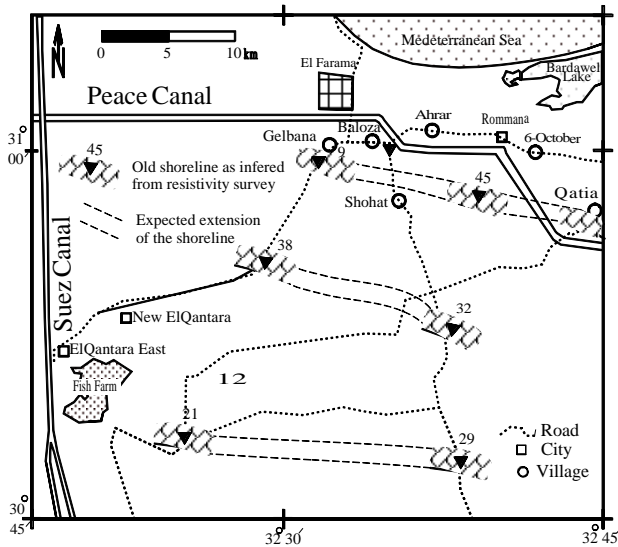


Figure 10. Relics of the old shore lines of the Mediterranean Sea as deduced from the geoelectric resistivity data.

At shallow depths, anomalous high resistive lenses ($\geq 700 \Omega \cdot m$) embedded with relatively low resistivity sediments (Figs. 4 and 7) with thickness ranging from 5.4 to 28m. These high resistive lenses are interpreted, on light of the calibration results, as a limestone conglomerate that represents the relics of the old shorelines of the Mediterranean Sea during its transgression during the Quaternary. Tracing of these high resistive zones along the geoelectric sections and the interpolation between such zones enable us to trace the old shoreline of the Mediterranean Sea that found more or less parallel to the present shoreline (Fig. 10). Surely, these limestone conglomerate beds are more abundant in the study area and can be traced accurately in the future by carrying out a detailed shallow geoelectric survey and coring.

CONCLUSIONS

Vertical electric resistivity soundings were conducted in northwestern Sinai to study the groundwater aquifers and the sedimentary facies that control them. In this respect 49 VESes were carried out along SW, SSE and EW profiles. In addition three VES stations were carried out close to three boreholes for assigning the geoelectric resistivity units to the corresponding lithologic units. The results indicate that there are three litho-resistivity units covered with a thin topmost layer of varied resistivities and an average thickness of about 0.4 m. The variation of resistivity of this layer is correlated with the variation in lithology that varies from aerated fine to coarse sand in the eastern and southern parts and to clay and silty clay in the northwestern parts of the study area. The first litho-resistivity unit is correlated with the shallow sand aquifer that attains resistivity values that decrease northwards due to increase in the salinity with

thicknesses decrease west- and northwards and increase southwards. The lowermost unit attains relatively higher resistivities that could be correlated to coarse sand and gravel saturated with fresh water could be originating from the deep Pliocene aquifer. The average depth of this deep aquifer is about 91 m. Along the study area, the shallow and deep sand aquifers are separated with a thick clayey unit that grades from clay to silty clay to sand clay attaining variable resistivities due to lithologic and hydrochemical changes. At shallow depths, anomalous high resistive lenses are embedded within these clayey sediments and are correlated to a limestone conglomerate that represents the relics of the old shoreline of the Mediterranean Sea shorelines.

REFERENCES

Ball J. (1939): Contribution to the Geography of Egypt. Survey Dep. Egypt Cairo, 300 pp

Diab, A. F. (1998): Geology, pedology and hydrogeology of the Quaternary deposits in Sahl El Tinah area and its vicinities for future development of north Sinai, Egypt. Ph. D. Thesis, Faculty of Science, Mansoura University, Egypt, 242pp.

ElHinnawi, M., Azer, A. and Aziz, M. (1994): Geologic map of Sinai, A. r. e. Sheet no. 5, Egyptian Geologic Survey and Mining Authority, scale 1:250,000.

ElSayed, A., Vaccari, F. and Panza (2001): Deterministic seismic hazards in Egypt. Geophysical Journal International, vol. 144, p. 1-20.

Ewieda, K. e., Laila, A. F. and Gamal, M. A. (1992): Groundwater conditions of Rommana – Bir ElAbd area, with emphasis on the area south of Rabaa village, north Sinai, Proceeding of 3rd Conference on the Geology of Sinai and Developments, Ismailia, 101 – 108.

Ibrahim, E. H.(1998): Credibility of using electric resistivity and seismic refraction in detecting Quaternary sedimentary variations ,Nile Delta, Egypt. Journal of Sedimentology of Egypt, 6., 129-140.

Inman, J. R.(1975): Resistivity inversion with ridge regression. Classic paper. Geophysics, 40, 798-817.

Neev, D. (1977): The Pelusiac Line a major transcontinental shear. Geophysics, T1-T8.

Shata, A. (1992): Watershed Management, Development of potential water resources and desertification control in Sinai. Proceeding of the 3rd Conference on the Geology and Development of Sinai. Ismailia, Egypt, 273 –280.

Stanley J. Daniel; James E. McRea, Jr., and John C. Waldron (1996): Nile Delta drill core and sample

database for 1985-1994: Mediterranean Basin (MEDIBA) Program. Smithsonian contribution to the marine sciences, 37, Smithsonian institution press. Washington, D. C. 428pp.

Zaghloul, Z. M., Taha, A. A., Hegab, O. A., and Fawal, F. (1979): The Plio-Pleistocene Delta environments, stratigraphic section and genetic class. Annual Meeting of the Geological Survey of Egypt, vol. 23, 282-291.

Zohdy, A. A. R (1989): A new method for the automatic interpretation of Schlumberger and Wenner sounding curves. Geophysics, 54, 2, 245-253.

Zohdy, A. and Besdorf, R. J. (1979): Programs for automatic processing and interpretation of Schlumberger sounding curves in Quick basic 4.0. Open-file report, 89-137 A&B.